



The effect of contrast polarity reversal on face detection: Evidence of perceptual asymmetry from sweep VEP



Joan Liu-Shuang^{a,*}, Justin M. Ales^b, Bruno Rossion^a, Anthony M. Norcia^c

^a Psychological Sciences Research Institute (IPSY) and Institute of Neuroscience (IoNS), University of Louvain, Belgium, 10 Place du Cardinal Mercier, 1348 Louvain-la-Neuve, Belgium

^b School of Psychology and Neuroscience, University of St-Andrews, Westburn Lane, St Andrews, Fife KY16 9JP, United Kingdom

^c Stanford Vision and NeuroDevelopment Lab, Department of Psychology, Stanford University, Jordan Hall, Building 420, Stanford, CA 94305-2130, USA

ARTICLE INFO

Article history:

Received 17 May 2014

Received in revised form 30 December 2014

Available online 13 January 2015

Keywords:

Face perception

Contrast reversal

EEG

SSVEP

Sweep VEP

Phase coherence scrambling

ABSTRACT

Contrast polarity inversion (i.e., turning dark regions light and vice versa) impairs face perception. We investigated the perceptual asymmetry between positive and negative polarity faces (matched for overall luminance) using a sweep VEP approach in the context of face detection (*Journal of Vision* 12 (2012) 1–18). Phase-scrambled face stimuli alternated at a rate of 3 Hz (6 images/s). The phase coherence of every other stimulus was parametrically increased so that a face gradually emerged over a 20-s stimulation sequence, leading to a 3 Hz response reflecting face detection. Contrary to the 6 Hz response, reflecting low-level visual processing, this 3 Hz response was larger and emerged earlier over right occipito-temporal channels for positive than negative polarity faces. Moreover, the 3 Hz response emerged abruptly to positive polarity faces, whereas it increased linearly for negative polarity faces. In another condition, alternating between a positive and a negative polarity face also elicited a strong 3 Hz response, indicating an asymmetrical representation of positive and negative polarity faces even at supra-threshold levels (i.e., when both stimuli were perceived as faces). Overall, these findings demonstrate distinct perceptual representations of positive and negative polarity faces, independently of low-level cues, and suggest qualitatively different detection processes (template-based matching for positive polarity faces vs. linear accumulation of evidence for negative polarity faces).

© 2015 Elsevier Ltd. All rights reserved.

1. Introduction

Human observers are extremely efficient at detecting faces in visual scenes (Crouzet, Kirchner, & Thorpe, 2010). Beyond low-level cues such as power spectrum (Crouzet & Thorpe, 2011; Keil, 2008) and the saliency of the eye regions (Paras & Webster, 2013), the nature of the visual information supporting face detection remains largely unknown. One critical element appears to be the contrast variation between different regions of a face. First noted by Galper (1970), the sensitivity of face perception to contrast polarity has been consistently observed (Bruce & Langton, 1994; Gilad, Meng, & Sinha, 2008; Johnston, Hill, & Carman, 1992; Kemp et al., 1996; Liu, Collin, & Chaudhuri, 2000; Liu et al., 1999; Nederhouser et al., 2007; Phillips, Jenkins, & Morris, 1972; Russell et al., 2006; Sormaz, Andrews, & Young, 2013; Vuong et al., 2005). However, these studies have focused on individual face recognition or discrimination and do not indicate to which

extent the weaker performance reflects an effect of contrast inversion on the perception of the stimulus as a face (i.e., face detection).

Studies that have addressed this question suggest that contrast polarity is fundamental to perceiving a face in a scene (Lewis & Edmonds, 2003, 2005). This observation is supported by developmental studies showing that contrast polarity is essential for face detection in newborns (Farroni et al., 2005) and older infants (Otsuka et al., 2012). From a neurofunctional point of view, in adults, there is an increased latency and amplitude of the face-sensitive N170 ERP component (Bentin et al., 1996; Rossion & Jacques, 2011 for a review) to negative polarity faces (Itier & Taylor, 2002; Tomalski & Johnson, 2012). In neuroimaging, the activation of face-selective regions such as the middle fusiform gyrus and, the anterior temporal cortex is reduced to negative polarity faces (George et al., 1999; Nasr & Tootell, 2012; Yue et al., 2013). Furthermore, face-selective cells in the monkey infero-temporal cortex decrease their firing rates to negative polarity faces (Ohayon et al., 2012 but see Rolls & Baylis, 1986). Taken together, these observations indicate that the basic perception of a face stimulus is altered by contrast polarity inversion, suggesting an asymmetry in the representation of facial features (i.e., eyes/eyebrows regions being

* Corresponding author. Fax: +32 10 47 37 74.

E-mail address: joan.liu@uclouvain.be (J. Liu-Shuang).

typically darker than the skin). However, studies that have applied contrast negation to face pictures have typically used Caucasian (i.e., white skin) faces, so that contrast negation reduced the overall luminance of the stimulus (Bruce & Langton, 1994; Galper, 1970; Nasr & Tootell, 2012; Itier & Taylor, 2002; Ohayon et al., 2012; Farroni et al., 2005; Itier, Latinus, & Taylor, 2006; Nederhouser et al., 2007; Otsuka et al., 2012; Russell et al., 2006; Vuong et al., 2005; Yue et al., 2013). Hence, the representation of positive and negative contrast faces is not directly comparable in the vast majority of studies (with the exception of the a few studies that controlled for luminance: George et al., 1999; Liu et al., 1999; Tomalski & Johnson, 2012). This is problematic because contrast inversion of low-level stimuli is typically assessed with stimuli that have equivalent white and black surfaces (i.e., symmetrical stimuli such as gratings or checkerboards). Therefore, the question of whether contrast polarity effects depend upon overall luminance or other low-level properties requires clarification.

Another outstanding issue is how contrast polarity influences face detection thresholds. Such thresholds have usually been investigated by parametrically varying stimulus visibility and measuring the behavioural and/or neural response functions using either functional magnetic resonance imaging (Jiang et al., 2011; Yue et al., 2013; Carlson, Grol, & Verstraten, 2006; James et al., 2000; Reinders, den Boer, & Büchel, 2005) or electroencephalography (EEG, Jemel et al., 2003; Philiastides, Ratcliff, & Sajda, 2006; Philiastides & Sajda, 2006; Rousselet et al., 2008; Schneider, DeLong, & Busey, 2007) and magnetoencephalography (MEG, Tanskanen et al., 2005). To our knowledge, none of these studies have compared face detection thresholds for positive and negative contrast polarity faces.

In EEG, the sweep Visual Evoked Potential (sweep VEP) technique (Regan, 1973) is particularly well suited to objectively and rapidly estimate perceptual response functions (Norcia & Tyler, 1985; Tyler et al., 1979; for review see Almoqbel, Leat, & Irving, 2008). With this approach, a stimulus is presented as a constant rate, (e.g., 4 images per second = 4 Hz) and evoking a high signal-to-noise ratio (SNR) periodic EEG response called the steady-state visual evoked potential (SSVEP; Regan, 1966, 1989). The SSVEP is quantified by transforming the EEG data in the frequency-domain and extracting the amplitude at the relevant frequency (e.g., 4 Hz). During a stimulation sequence, a stimulus parameter is varied or “swept” parametrically (e.g., spatial frequency, Norcia & Tyler, 1985; contrast, Norcia, Tyler, & Hamer, 1990). This allows one to estimate the perceptual threshold by regressing the SSVEP response amplitude to zero and to examine the supra-threshold response function. These SSVEP responses are objectively identified because they occur exactly at the frequency defined by the experimenter.

Here we use a variation of the typical sweep VEP approach in which two streams of stimuli (A and B) alternate, with one stream remaining constant (stream A) while the other stream (stream B) parametrically varies (e.g., Vernier offset, Hou, Good, & Norcia, 2007; orientation-defined structure, Pei, Pettet, & Norcia, 2007). The visual system generates a specific response to every other stimulus if and when it differentiates between the two streams. In terms of the SSVEP, this asymmetry translates into a periodic response exactly at half the image presentation rate, or at the presentation rate of a single stream (i.e., $4\text{ Hz}/2 = 2\text{ Hz}$).

In a recent study, Ales et al. (2012) used this structure-related sweep VEP to measure face detection thresholds by gradually increasing phase coherence of face images. The image stream containing faces was presented in alternation with a stream of fully phase-scrambled images at a rate of 6 Hz and face detection was indexed by periodic EEG responses at the presentation rate of face images, i.e., 3 Hz. In this study, the 3 Hz response emerged abruptly at around 30% coherence on right occipito-temporal channels,

where face-specific EEG responses to transient stimulation (i.e., N170; Bentin et al., 1996; Rossion & Jacques, 2011) or periodic stimulation (Rossion & Boremanse, 2011) are typically found.

To investigate the role of contrast polarity in face perception, we built upon this validation study and compared threshold and supra-threshold responses to positive and negative contrast polarity faces that were equated for low-level visual properties (i.e., power spectrum). Based on previous studies, we predicted higher thresholds and reduced 3 Hz (1F) amplitudes for a negative polarity face. In a third condition, we directly measured the asymmetry between positive and negative polarity faces by alternating streams of positive and negative polarity faces. In this polarity reversal condition, a 1F response should emerge if and when the representation of faces with opposite polarities differ.

2. Experiment 1

2.1. Methods

2.1.1. Participants

We tested 10 adult participants (age range = 20–58, mean age = 36.5 ± 11.5 , see Supplementary Table for exact ages), with normal or corrected-to-normal vision. All gave written informed consent according to the guidelines of the Institutional Review Board of Stanford University and in accordance with the Code of Ethics of the World Medical Association (Declaration of Helsinki).

2.1.2. Stimuli

Stimuli were part of the set used in Ales et al. (2012) and further details regarding their creation can be found in that paper. To summarise, the power spectra of a set of greyscale faces were equalised and the faces were smoothly embedded in a background composed of the phase-scrambled average power spectrum. A sequence of 20 images was generated by parametrically varying the phase coherence of the embedded faces from 0% to 100% in 5.26% equal steps. Hence, in a sweep sequence, the face gradually appeared in a scrambled background over 20 steps (Fig. 1A). Complementary sequences that did not contain faces were generated by fully phase-scrambling the average power spectrum. For both face and scrambled sequences, the phase scrambling at each step was newly randomised. For the current experiments, we selected one sequence containing a full-frontal female face with a neutral expression (20 images) and a phase-scrambled sequence (40 images). Negative contrast polarity versions of these images were generated by inverting the contrast around the mean luminance value (Fig. 1A, bottom). The image dimensions were 512×512 pixels and subtended 11.44° of visual angle at a distance of 127 cm. Stimuli were shown on a 800×600 pixels CRT screen with a 72 Hz refresh rate.

2.1.3. Procedure

The experiment consisted of four conditions in which face and scrambled images alternated at a rate of 3 Hz (presentation rate = 6 images per second). If there is no perceptual asymmetry (i.e., no difference between images), this stimulation typically evokes a periodic EEG response *only* at the presentation rate (second harmonic: $2F = 6\text{ Hz}$). However, an asymmetry should lead to a response also at the reversal rate (first harmonic: $1F = 3\text{ Hz}$). Hence, the 1F response indexes the discrimination between face and scrambled images.

In the first two conditions, positive and negative polarity face images were alternated with phase-scrambled images (Fig. 1B). The 20 levels of coherence were shown for 1 s each. Crucially, a different scrambled image was presented for each level of face image coherence so that there were 40 different images in total per

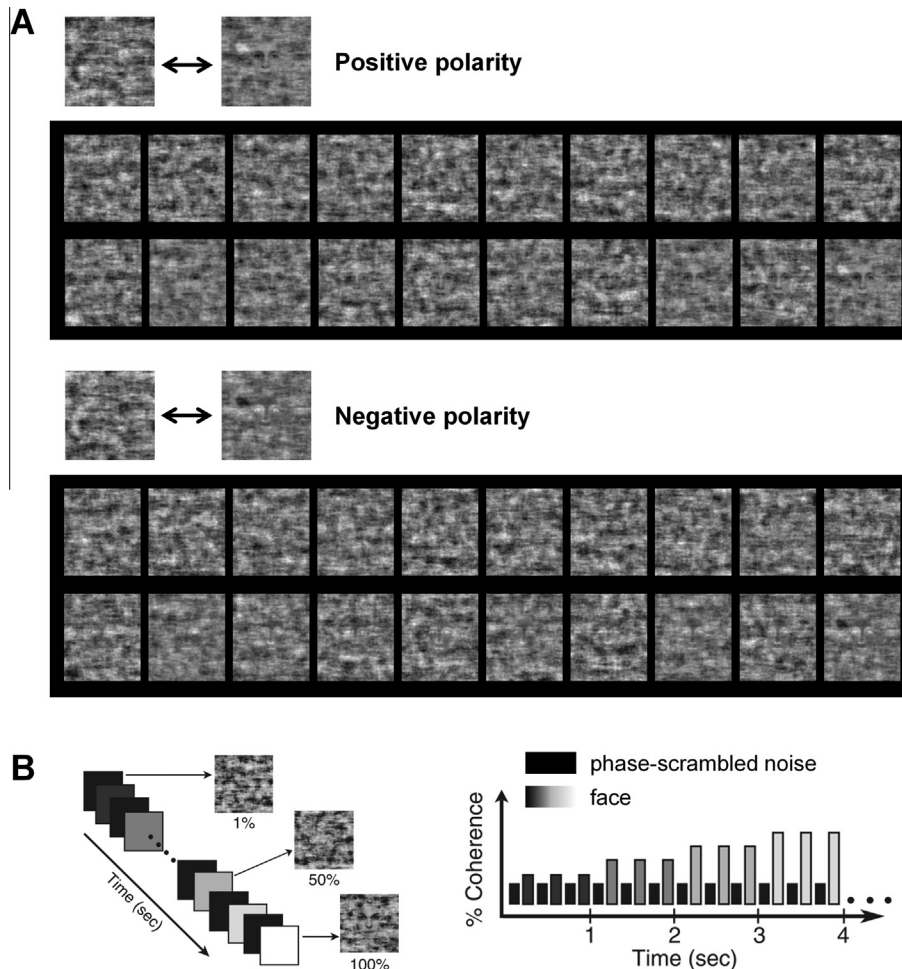


Fig. 1. (A) Face stimuli: the phase-coherence of a centrally located face gradually increases in 20 steps, so that a face slowly emerges against a phase-scrambled background. (B) Schematic illustration of a sweep sequence in which 100% phase-scrambled images alternate with the face stimuli (left panel). The phase coherence of the noise images (black bars) remains at 0% throughout the sequence whereas the coherence of the face images (greyscale bars) increases from 0% to 100% in 5.26% steps (right panel).

sequence (20 face images and 20 scrambled images). These two conditions were used to measure the effect of contrast polarity reversal on neural face detection thresholds. A 3rd condition that only contained phase-scrambled images served as baseline. A 4th condition aimed to quantify the asymmetry between contrast polarities by alternating between a positive and a negative polarity face (polarity reversal). Hence, a face gradually emerged in both image streams but one appeared in positive polarity and the other in negative polarity (Fig. 3A).

All conditions lasted 20 s and were flanked by a 1-s repetition of the first and last steps in order to exclude potential transient ERP responses. There were 15 random repetitions of each condition during the experiment for a total test duration of 28 min. Participants were instructed to fixate on a central cross and to maintain attention during the entire trial.

2.1.4. EEG acquisition

EEG data was recorded using a 128-channel Hydrocell Geodesic Sensor Net (Electrical Geodesics Inc., Eugene, OR, USA) at a sampling rate of 500 Hz. Electrode impedances were adjusted below 60 k Ω prior to recording. The data was then band-pass filtered (0.3–50 Hz, 0.3 Hz slope) offline with the NetStation Filtering Tool (Kaiser type FIR filter), resampled to 432 Hz and inspected for artefacts using a custom software (PowerDiva). In the first step of artefact rejection, channels containing more than 15% of datapoints exceeding a threshold of 30 μ V during the entire recording were

replaced by the average of their six neighbouring channels and EEG data was re-referenced to the average of all channels. The second step of artefact rejection consisted in excluding 1 s epochs on a channel-by-channel basis if they contained more than 10% of samples exceeding 30 μ V. Entire epochs were rejected if they contained blinks (more than 7 channels exceeding 60 μ V).

2.1.5. SSVEP analysis

Steady-state visual evoked potentials (SSVEPs) were analysed in two ways. First, a discrete Fourier transform analysis was applied to the data to extract the amplitudes of the overall SSVEP responses in each condition. Second, data from each step of the sweep sequence were analysed with a Recursive Least Squares (RLS) filter in order to measure the response amplitude as a function of stimulus coherence (Tang & Norcia, 1995). Compared to computing a discrete Fourier transform analysis on each step separately, the RLS method adaptively estimates the response phase from the data, with a resulting improvement of SNR of 3 dB (Tang & Norcia, 1995).

In order to describe the response amplitude vs. coherence function, we fit a step and a hinge function to the data using a non-linear least-square curve fitting algorithm (Levenberg–Marquardt) as implemented by the `curve_fit` method in the `scipy` Python toolbox. The step function was defined as a function that abruptly increases from one constant value to another at a certain value of x . The hinge function was defined as a continuous piecewise linear func-

tion made of two parts that transition at a certain value of x , the first one being constant and the second one being linearly increasing. The fit errors (root mean squared errors, RMSE) of each function were extracted separately for each individual participant then averaged per condition. The smaller the error value, the better the fit of the function.

2.1.6. Creation of predicted polarity reversal dataset

To better understand the results in the polarity reversal condition, we compared the real dataset with an artificial dataset created based on the prediction that the 1F response in the polarity reversal condition would be the linear difference between the positive and negative face conditions. This predicted dataset was computed differently for the 1F and 2F responses. The predicted 1F response was the difference between the 1F response in the positive polarity condition and the negative polarity condition, added to a baseline value (reflecting background EEG noise) that was the mean amplitude of two adjacent frequencies (2.5 and 3.5 Hz) averaged across the entire sweep. Negative values were set to zero. The predicted 2F responses was the average amplitude of positive and negative polarity conditions, since the low-level visual processing should not vary between conditions.

2.1.7. 1F response threshold estimation

To determine the coherence level at which the 1F response emerged from the background EEG noise, we first estimated signal and noise with integrated response functions (see Ales et al., 2012). Signal was the cumulative sum of the amplitudes at the first harmonic (3 Hz) whereas noise was the cumulative sum of the mean noise during the trial (average amplitude of two neighbouring frequencies, 2.5 and 3.5 Hz). The cumulative amplitudes were normalised to the maximum value of the signal. A hinge function was then fitted to the difference between the normalised signal and noise functions and the 1F response onset was defined as the inflection point of the hinge function. In case of unrealistic negative values or if the difference between signal and noise was negative or had a negative slope, the threshold was set to 100% coherence (no face detection).

2.2. Results

2.2.1. Positive vs. negative polarity face sweep

Fig. 2 depicts the results from the positive and negative polarity face sweeps. Considering the overall response across the entire 20-s stimulation sequence, there is a second harmonic (2F = 6 Hz) response centred on medial occipital channels of comparable amplitude in all face and scrambled conditions (Fig. 2A and B, middle row, Supplementary Fig. 1). However, the first harmonic (1F = 3 Hz) response, reflecting the perceived difference between face and scrambled images, is present only in the face conditions (Bonferroni-corrected p s < 0.00002; 0.12–0.94 μ V). There are only minor 1F responses in the scrambled condition (0.11–0.14 μ V; Supplementary Fig. 1), which fall within rates predicted by Type I error and will not be analysed further. The 1F responses in the face conditions have a broad posterior topography, extending from the medial occipital region to lateral occipital sites, with a right hemisphere dominance (Fig. 2A and B). In order to quantify face-related response, we computed an index of the 1F response (1F/(1F + 2F), see Ales et al., 2012; Fig. 2B). A higher index indicates that the total evoked response, normalised for overall magnitude, contains a higher proportion of response due to face-related processing. Conversely, a lower index indicates that the total evoked response reflects non-specific low-level visual processing. As can be seen in Fig. 2A (bottom row), the 1F index peaks over bilateral occipito-temporal regions and its right lateralisation appears larger for positive polarity faces (7/10 participants) than negative polarity

faces (4/10 participants; Fig. 2A, bottom row; Supplementary Fig. 2). The medial occipital region exhibits the lowest 1F index values. This topographical dissociation between frequencies is consistent with the 2F response reflecting the modulation of low-level visual features in the stimuli, while the 1F response reflects high-level processes (i.e., perceptual face detection, see Ales et al., 2012).

Based on the distinctive topography of the 1F index values, we focused on three regions-of-interest (ROIs) to conduct further statistical comparisons between 1F and 2F responses: right occipito-temporal (rOT, channels 95, 96, 97, 100, 101), left occipito-temporal (lOT, channels 50, 51, 57, 58, 64), and medial occipital (Occ, channels 70, 71, 72, 75, 76, 83) (see Fig. 2B, top right for the channels composing these ROIs). We separately analysed 1F and 2F responses with repeated measures ANOVAs using the conditions and their respective relevant ROIs as within-subject factors.

First, a 3×2 repeated measures ANOVA on the 1F response with Condition (positive faces, negative polarity faces, scrambled) and ROI (lOT vs. rOT) as within-subject factors showed significant effects of Condition ($F(2, 18) = 19.32, p < 0.0001, \eta^2 = 0.68$) and ROI ($F(1, 9) = 119.60, p < 0.002, \eta^2 = 0.68$), with a significant Condition \times ROI interaction ($F(2, 18) = 4.52, p = 0.026, \eta^2 = 0.33$). Consistent with our above observations, the amplitude of the 1F response was larger for positive compared to negative polarity faces ($t(9) = 4.31, p < 0.006$, Bonferroni-corrected, mean difference = 0.19, 95% CI = [0.09, 0.29], 10/10 participants), and was larger for both face conditions compared to the scrambled condition (positive polarity faces: $t(9) = 5.48, p < 0.001$, mean difference = 0.52, 95% CI = [0.30, 0.73]; negative polarity faces: $t(9) = 3.19, p < 0.033$, mean difference = 0.32, 95% CI = [0.10, 0.55], Bonferroni-corrected, both in 10/10 participants). Overall, responses were larger in the right than the left occipito-temporal ROI (mean difference = 0.12, 95% CI = [0.06, 0.18], 9/10 participants). Finally, the Condition \times ROI interaction shows a stronger right lateralisation for positive polarity faces ($t(9) = 3.28, p < 0.03$, Bonferroni-corrected, mean difference = 0.24, 95% CI = [0.07, 0.40], 8/10 participants) than for negative polarity faces (which did not survive multiple comparison correction: $t(9) = 2.39, p = 0.12$, Bonferroni-corrected). There were no differences between ROIs in the scrambled condition ($t(9) = 1.08, p = 0.93$). Second, a 3-way repeated measures ANOVA on the 2F response in the occipital ROI with Condition (positive polarity, negative polarity, baseline) as within-subject factor did not reveal any significant effects ($F(1.03, 9.28) = 0.8, p = 0.4, \eta^2 = 0.08$). Hence, the basic low-level visual response was comparable across conditions. The scrambled condition will not be further analysed.

Next, we examined the profile of the 1F and 2F responses across coherence levels. Fig. 2C shows the amplitude of the 1F and 2F response in each ROI, plotted as a function of the coherence of the face stimuli. The 1F responses systematically increase in amplitude as coherence increases, but the 2F response amplitudes remained constant. Furthermore, the 1F responses to positive and negative polarity faces differ in their profiles (a step-like increase with a plateau for positive polarity faces compared to a linear increase until the end of the sequence for negative polarity faces), as well as in their apparent onset ($\approx 30\%$ of stimulus coherence for positive polarity faces vs. $\approx 40\%$ for negative polarity faces, in the right occipito-temporal ROI).

In order to quantify these differences, we first tested which of two functions, a step or a hinge function, best accounted for the response profiles. The results summarised in Table 1 indicate that a step function best fits the response profile of positive polarity faces whereas the hinge function best fits for negative polarity faces. We statistically verified this pattern with a $2 \times 2 \times 2$ repeated measures ANOVA with Condition (positive vs. negative polarity), Function (step vs. hinge), and ROI (rOT vs. lOT) as within-subject factors, which revealed main effects of Condition

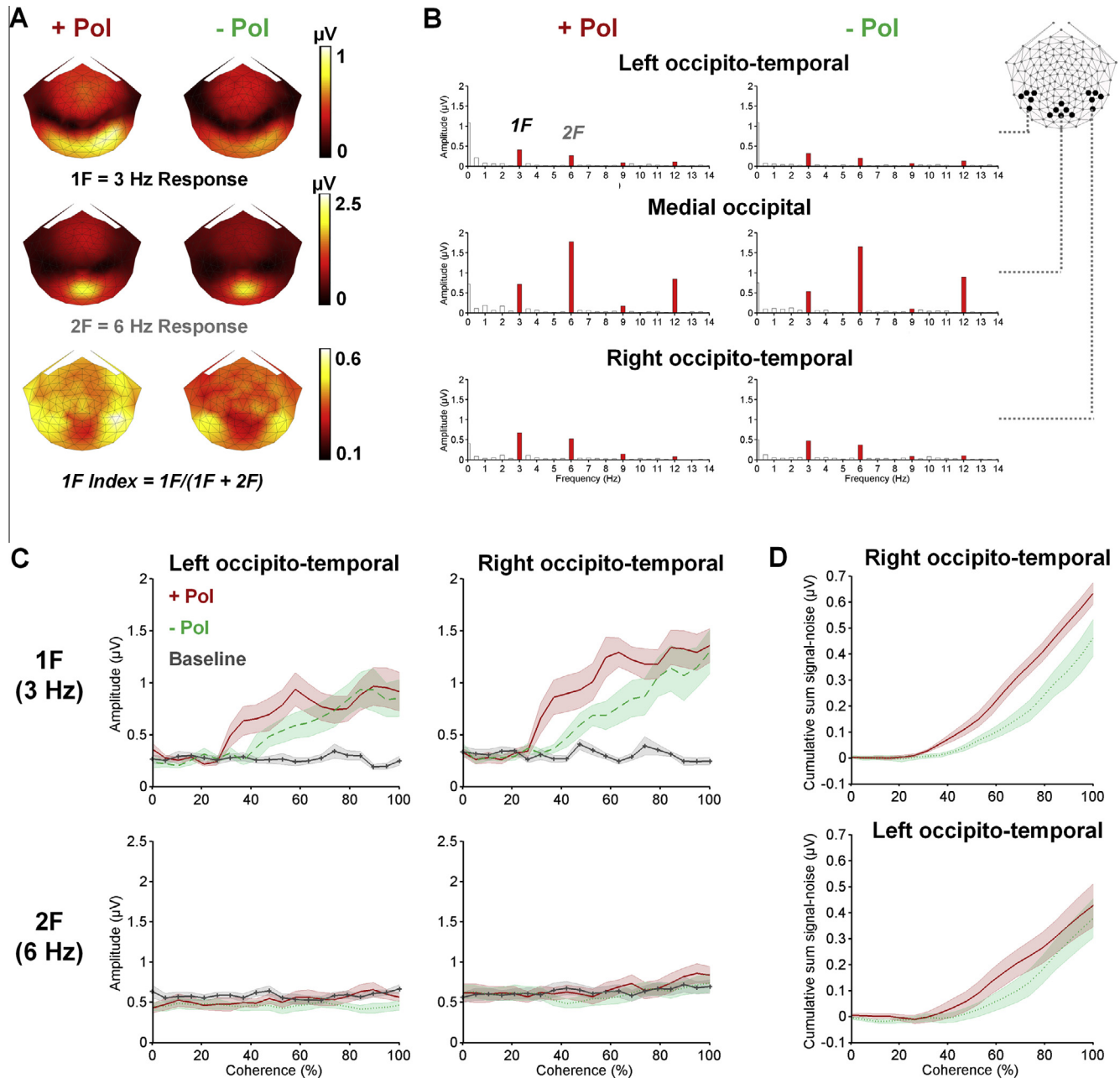


Fig. 2. Results for positive and negative polarity face sweeps. (A) Topographical distributions of the 1F amplitude (top row), 2F amplitude (middle row), and 1F Index (bottom row) for positive (left) and negative (right) polarity faces. (B) Frequency spectra of the periodic responses in the three regions-of-interest (channels composing these ROIs are shown on the schematic on the top right) for positive (left) and negative (right) polarity faces. (C) 1F and 2F responses as a function of percent coherence of the face image, in each ROI for positive and negative polarity faces, as well as a 100% phase-scrambled condition. (D) Mean difference of normalised cumulative signal and noise functions for positive and negative polarity faces. The shaded regions represent the SEM. +Pol = positive polarity; -Pol = negative polarity.

Table 1

Mean root mean squared errors (RMSE) values (SEM) of step and hinge functions fitted to the 1F response functions from the bilateral occipito-temporal ROIs for each condition.

	IOT		rOT	
	Step	Hinge	Step	Hinge
+Pol	0.64 (0.09)	0.75 (0.12)	0.76 (0.09)	1.02 (0.14)
-Pol	0.63 (0.09)	0.59 (0.07)	0.79 (0.12)	0.59 (0.07)
Pol Rev	0.68 (0.11)	0.80 (0.14)	0.83 (0.09)	0.93 (0.13)
Pred Pol Rev	0.85 (0.11)	0.91 (0.12)	1.07 (0.12)	1.25 (0.15)

Lower values mean a better fit with the respective function. +Pol = positive polarity faces; -Pol = negative polarity faces; Pol Rev = polarity reversing faces. rOT = right occipito-temporal region; IOT = left occipito-temporal region.

($F(1, 9) = 11.46$, $p < 0.008$, $\eta^2 = 0.56$) and ROI ($F(1, 9) = 7.75$, $p < 0.021$, $\eta^2 = 0.46$), as well as a significant Condition \times Function interaction ($F(1, 9) = 7.39$, $p < 0.024$, $\eta^2 = 0.45$). There was also a marginal Condition \times ROI \times Function triple interaction ($F(1, 9) = 5.10$, $p = 0.05$, $\eta^2 = 0.36$). The functions fit better for negative than for positive polarity faces (mean difference = -0.14 , 95% CI = $[0.23, 0.05]$, 8/10 participants) and the fit was better in the left compared to the right occipito-temporal ROI (mean difference = 0.14 , 95% CI = $[0.30, 0.26]$, 8/10 participants). The Condition \times Function interaction indicated qualitatively different response profiles (though they did not reach threshold corrected for multiple comparisons): the step function tended to be the best fit for positive polarity faces ($t(9) = -2.24$, $p = 0.05$, Bonferroni-cor-

rected, mean difference = -0.18 , 95% CI = $[-0.36, 0.002]$, 8/10 participants), while the hinge function tended to be the best fit for negative polarity faces ($t(9) = 1.78$, $p = 0.11$, Bonferroni-corrected, mean difference = 0.12 , 95% CI = $[-0.03, 0.27]$, 6/10 participants). Based on the trend for a Condition \times ROI \times Function interaction, this was especially true in the right occipito-temporal ROI (positive polarity faces: $t(9) = -2.59$, $p < 0.015$, mean difference = -0.25 , 95% CI = $[-0.47, -0.03]$; negative polarity faces: $t(9) = 2.60$, $p < 0.015$, mean difference = 0.20 , 95% CI = $[0.03, 0.37]$; in 8/10 participants in both cases).

We then calculated the coherence threshold of the 1F response in both conditions using cumulatively summed signal and noise functions (see methods for details). Table 2 summarises the mean thresholds in each condition and Supplementary Fig. 3 shows the individual participant data. Results confirm the visually estimated threshold differences. Positive polarity faces evoked 1F responses at lower coherence values ($\approx 38\%$) compared to negative polarity faces ($\approx 56\text{--}59\%$). A repeated measures ANOVA with Condition and ROI as within-subject factors showed only a significant main effect of Condition ($F(1, 9) = 36.86$, $p < 0.001$, $\eta^2 = 0.80$). The onset of the 1F face-related response occurred at a significantly lower coherence level for positive than negative polarity faces (mean difference = -14.47 , 95% CI = $[-21.83, -7.15]$, 10/10 participants).

2.2.2. Polarity reversal face sweep

Based on the observation that positive contrast faces evoked larger 1F responses than negative contrast faces, we reasoned that an alternation between a positive and negative polarity face (see Fig. 3) would lead to a 1F response that would be largest at the coherence levels at which the amplitude difference between contrast polarities was the largest (i.e., 30–70%). In other words, the 1F response should reflect steps at which the perception of positive and negative polarity faces is the most dissimilar. However, the 2F response should remain stable, given that the low-level visual properties of the faces were equalised and processed similarly (see above). We created an artificial dataset based on these predictions and compared it with the real data from the polarity reversal sweep.

The real data from the polarity reversal sequences did show significant 1F responses (Bonferroni corrected $ps < 0.00002$; $0.12\text{--}0.54 \mu\text{V}$), thus reflecting an asymmetry in the perception of positive and negative polarity faces (Fig. 4A). Consistent with the predicted data, the topography of the real 1F response was right lateralised on occipito-temporal channels, while the 2F response was centred on medial occipital channels (Fig. 4B). This was further underlined by the 1F index results (Fig. 4B, right). However, the 1F response amplitude was larger in the real than the predicted data, while there were no differences at 2F. A 2×2 repeated measures ANOVA on the 1F responses with Dataset (real vs. predicted) and ROI (rOT vs. lOT) as within-subject factors supports this observation. Results show main effects of Dataset ($F(1, 9) = 9.45$, $p < 0.013$, $\eta^2 = 0.51$, mean difference = 0.25 , 95% CI = $[0.07, 0.43]$, 8/10 participants) and ROI ($F(1, 9) = 5.81$, $p < 0.039$, $\eta^2 = 0.39$, mean

difference = 0.14 , 95% CI = $[0.01, 0.27]$, 7/10 participants), but no Dataset \times ROI interaction ($F(1, 9) = 0.025$, $p = 0.88$, $\eta^2 = 0.003$). Conversely, a two-way repeated measures ANOVA on the 2F responses in the occipital ROI with Dataset (real vs. predicted) as within-subjects factor did not reveal any significant differences ($F(1, 9) = 0.16$, $p = 0.70$, $\eta^2 = 0.02$).

We examined this discrepancy in the 1F response amplitude with the predicted and real sweep response functions (Fig. 4C). While the 2F response function remained stable across all coherence levels in both predicted and real datasets, we observed differences between the predicted and real 1F response profiles around the higher coherence levels ($\approx 70\text{--}100\%$). However, the actual onset of 1F responses across datasets was step-like (see Table 1) and at comparable coherence levels (see Table 2). The response profile similarities between predicted and real data was verified with a $2 \times 2 \times 2$ repeated measures ANOVA with Dataset (real vs. predicted), Function (step vs. hinge), and ROI (rOT vs. lOT) as within-subject factors. There were main effects of Dataset ($F(1, 9) = 5.63$, $p < 0.042$, $\eta^2 = 0.38$, mean difference = -0.21 , 95% CI = $[-0.71, -0.01]$, 8/10 participants) and ROI ($F(1, 9) = 8.15$, $p < 0.019$, $\eta^2 = 0.48$, mean difference = 2.09 , 95% CI = $[0.04, 0.38]$, 9/10 participants), indicating that the functions were better fitted for the real compared to the predicted dataset and that fits were better in the left compared to the right occipito-temporal ROI. Critically, there was a main effect of Function ($F(1, 9) = 11.04$, $p < 0.009$, $\eta^2 = 0.55$, mean difference = -0.11 , 95% CI = $[-0.19, -0.04]$, 8/10 participants) because both datasets were better described by step functions, without any significant interactions.

The estimated 1F response thresholds are summarised in Table 2. The statistical comparison of the thresholds with a 2×2 repeated measures ANOVA with Dataset (real vs. predicted) and ROI (rOT vs. lOT) as within-subject factors did not show any significant main effects nor interactions, thus indicating that the onset of the 1F response was equivalent in both predicted and real polarity reversal conditions. Note that the threshold in the polarity reversal condition occurs around the same coherence level as the positive polarity face sweep (i.e., $\approx 35\%$).

We further analysed the supra-threshold differences between the predicted and real 1F responses to the polarity reversing faces by conducting pairwise permutation tests between the two datasets at each coherence level (1024 permutations, p -value threshold = 0.05). A cluster-based correction for multiple comparisons was applied (Maris & Oostenveld, 2007). Significant differences between datasets are illustrated in Fig. 4C. Globally, the real 1F response amplitude was larger than the predicted values from $\approx 74\%$ until $\approx 100\%$ of coherence (uncorrected range). Using the cumulative sum approach (see Section 2.1), we then estimated the exact coherence level at which real and predicted data began deviating. More precisely, we calculated the cumulatively summed amplitudes for the real and predicted data then normalised the values according to the maximum value of the real data. The difference between normalised amplitudes was fitted with a hinge function and the inflection point extracted. Real 1F responses began to deviate from our linear prediction at approximately 60% coherence (rOT = $56.94 \pm 6.88\%$; lOT = $55.37 \pm 8.72\%$). Interestingly, this corresponds to the onset of the 1F face detection response in the negative polarity condition (see Table 2).

2.3. Summary of Experiment 1

We found asymmetrical (face detection) responses both for positive and negative polarity faces. These first harmonic (1F) responses were observed over bilateral occipito-temporal channels with a right hemisphere lateralisation, which correspond to the typical topography of face-related responses reported in the literature. The 1F response amplitude across coherence levels revealed

Table 2
Thresholds of 1F response onset in terms of percent of phase coherence (SEM) in occipito-temporal ROIs.

	lOT	rOT
+Pol	38.35 (3.74)	37.64 (3.48)
−Pol	59.07 (5.73)	56.40 (5.72)
Pol Rev	32.74 (5.60)	34.13 (5.20)
Pred Pol Rev	47.56 (12.71)	51.30 (11.43)

+Pol = positive polarity faces; −Pol = negative polarity faces; Pol Rev = polarity reversing faces; Pred Pol Rev = predicted values for polarity reversing faces (+Pol − Pol). rOT = right occipito-temporal region; lOT = left occipito-temporal region.

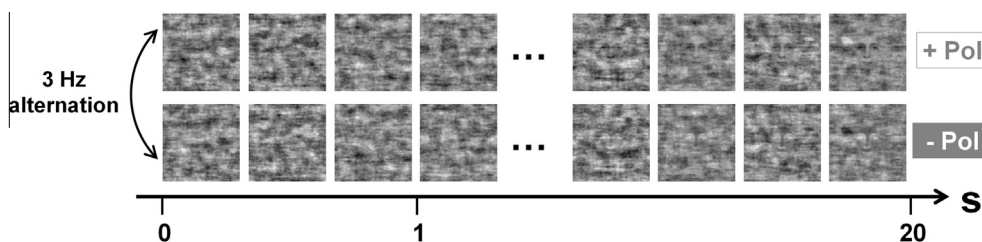


Fig. 3. Schematic illustration of the polarity reversal sequence. The sweep sequence containing a positive polarity face was alternated with the sweep sequence containing a negative polarity face at a rate of 3 Hz so that a face was progressively revealed in both stimulus streams.

quantitative (coherence threshold) and qualitative (response function) differences between polarities. This observation suggests an asymmetry between the perceptual representation of a positive and a negative contrast polarity face, even when low-level cues are controlled for. This is further supported by the presence of an asymmetrical evoked response when positive and negative polarity face images alternate with each other. If the difference between opposite polarity faces only involved the rate of evidence accumulation, we predicted that the asymmetrical 1F response would disappear at supra-threshold levels. However, the 1F response to polarity reversing faces was sustained throughout the sweep sequence. Additionally, this response bore a strong resemblance to the response for positive polarity faces both in terms of the onset and profile of the response.

3. Experiment 2

The purpose of Experiment 2 was to replicate the findings for the polarity reversal condition in Experiment 1 and to test whether there are image statistics (intermediate-level features) not related to face structure that contribute to the asymmetrical response. Using contrast-reversing checkerboards that only elicit 2F responses as a baseline, we measured 1F responses to stimuli in which the amount of face-specific image properties were varied by either keeping only the power spectrum information or the power spectrum and some elementary shape/shading and edge properties (using the texture synthesis algorithm by Portilla & Simoncelli, 2000). Thus, the four conditions were contrast-reversing checkerboards (baseline condition), phase-scrambled stimuli (low-level face structure condition), texture-scrambled stimuli (mid-level face structure condition), and faces (polarity reversal condition of Experiment 1).

3.1. Methods

3.1.1. Participants

We tested 10 adult participants (age range = 21–61, mean age = 30.6 ± 12.5 , see Supplementary Table for individual participant ages), with normal or corrected-to-normal vision. One participant had also completed Experiment 1. All gave written informed consent according to the guidelines of the Institutional Review Board of Stanford University and in accordance with the Code of Ethics of the World Medical Association (Declaration of Helsinki).

3.1.2. Stimuli and procedure

Four types of stimuli were used in this experiment: checkerboards, phase-scrambled images, scrambled images based on a texture synthesis algorithm (Portilla & Simoncelli, 2000), and faces (Fig. 5). Checkerboard stimuli were composed of 8×8 alternating black and white squares. The phase-scrambled sequence consisted of 20 differently scrambled images. A set of 20 texture-scrambled images based on the face stimulus were created using the Portilla and Simoncelli (2000) algorithm (4 scales and orientations,

spatial neighbourhood = 9). This algorithm calculates image statistics so that the output image is matched not only on low-level contrast and spatial frequency content of the original image but also on a set of joint statistics over scale, orientation and space, corresponding to mid-level shape, shading and edge properties. The power spectrum of these images was equalised to the spectrum of face images using the SHINE toolbox (Willenbockel et al., 2010). Finally, the sequence of 20 gradually emerging face stimuli was identical to Experiment 1. Negative polarity counterparts of each type of stimulus were created by inverting the positive polarity images' luminance histogram around the mean value of 127 (see Fig. 5, bottom row). All histograms were sufficiently symmetrical that there was no perceivable flicker during contrast reversal. The image dimensions were 512×512 pixels and subtended 11.44° of visual angle at a distance of 127 cm. Stimuli were shown on a 800×600 pixels CRT screen with a 72 Hz refresh rate.

Each stimulus condition was presented by alternating its positive and negative polarity versions at a rate of 3 Hz (6 images per second) for 20 s. For the phase- and texture-scrambled and face conditions, the image content changed every second of the 20 s sequence, while the pair of checkerboards remained constant. There were 15 random repetitions of each condition during the experiment for a total test duration of 28 min. Participants were instructed to fixate on a central cross and to maintain attention during the entire trial.

3.1.3. EEG acquisition and SSVEP analysis

EEG acquisition and analysis methods were identical to Experiment 1.

3.2. Results

The topographies and frequency spectra of 1F and 2F responses are shown on Fig. 6. As in Experiment 1, significant 2F responses were found in all conditions. The spatial distribution of the 2F response was consistent across conditions, again supporting the interpretation that this 2F response mainly captures low-level visual processing. A repeated measures ANOVA on the 2F response amplitudes in the medial occipital ROI with Condition (checkerboard, phase-scrambled, texture-scrambled, face) as within-subjects factor revealed a significant effect ($F(1.43, 12.9) = 10.04$, $p < 0.004$, $\eta^2 = 0.53$). Post-hoc comparisons (Bonferroni-corrected) show that checkerboards evoked larger responses than texture-scrambled ($p < 0.04$, mean difference = 0.59, 95% CI = [0.03, 1.15], 8/10 participants) and face stimuli ($p < 0.02$, mean difference = 0.69, 95% CI = [0.12, 1.27], 9/10 participants) but not than phase-scrambled stimuli ($p = 0.11$, mean difference = 0.59, 95% CI = [-0.01, 1.29]).

There were no 1F responses above EEG noise level for contrast reversal of the checkerboard and phase-scrambled images, consistent with the lack of high-level structure modulation. Contrast-reversing faces elicited strong 1F activity (Bonferroni-corrected $ps < 0.00002$; range = 0.1–0.73 μV) peaking on right occipito-temporal channels, replicating results from Experiment 1 (Fig. 6 and

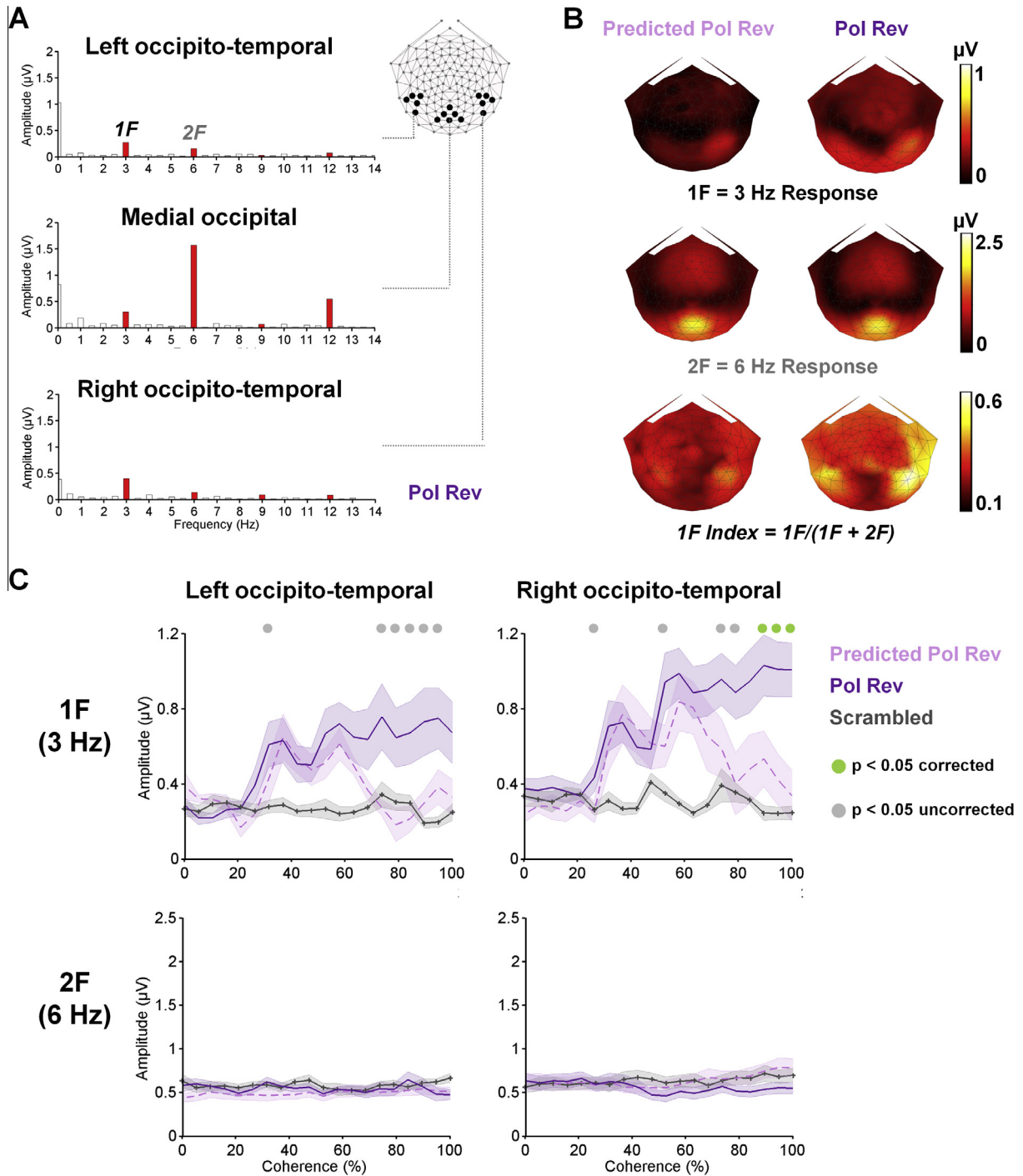


Fig. 4. Results for polarity reversal face sweep. (A) Frequency spectra of the periodic responses in the real dataset shown for the three regions-of-interest (channels composing these ROIs are shown on the schematic on the top). (B) Predicted (left) and real (right) topographical distributions of the 1F amplitude (top), 2F amplitude (middle), and 1F index (bottom). (C) Predicted (dotted) and real (solid) 1F and 2F response sweep response functions for polarity reversing faces, overlaid with the scrambled condition as reference. Significant differences between predicted and real 1F responses are indicated by the dots. The shaded regions represent the SEM. Pol Rev = polarity reversal.

Supplementary Fig. 4. Weak but significant 1F responses (Bonferroni-corrected $p_s < 0.00002$; range = 0.11–0.21 μV) were found for texture-scrambled stimuli on the medial occipital region.

We computed an index of 1F responses for the conditions with 1F responses. The topographies of the 1F indexes underline the contribution of bilateral occipito-temporal regions in generating the polarity-specific responses (Fig. 7). Similarly to Experiment 1,

we concentrated on these ROI for further analysis. A 2×2 repeated measures ANOVA on the 1F response amplitude with Condition (texture-scrambled vs. faces) and ROI (rOT vs. lOT) as within-subject factors revealed a main effect of Condition ($F(1, 9) = 16.43$, $p < 0.003$, $\eta^2 = 0.65$, mean difference = 0.25, 95% CI = [0.11, 0.38], 9/10 participants) due to larger asymmetrical responses for faces than for texture-scrambled stimuli. There was no effect of ROI

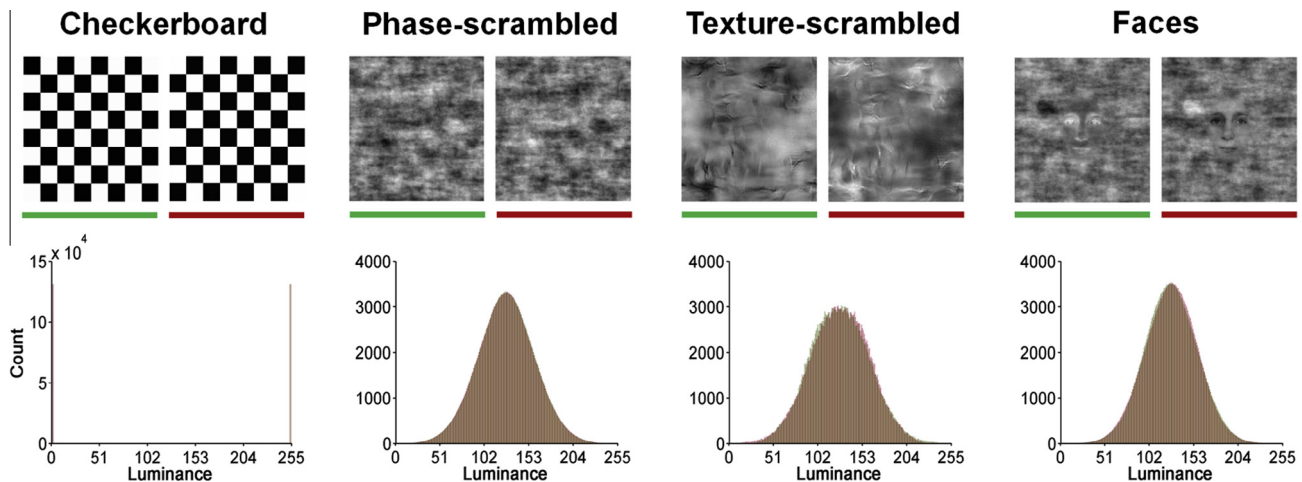


Fig. 5. Luminance histograms of the positive and negative polarity images in each condition. In all conditions, the histograms are symmetrical and centred around the mean background luminance value of 127.

($F(1, 9) = 0.24$, $p = 0.64$, $\eta^2 = 0.026$, mean difference = 0.02, 95% CI = [-0.7, 1.11]) nor any Condition \times ROI interaction ($F(1, 9) = 2.08$, $p = 0.18$, $\eta^2 = 0.19$).

To summarise, findings from Experiment 2 replicate the asymmetrical contrast polarity reversal response from Experiment 1. Furthermore, while stimuli with the same power spectrum as faces did not elicit any 1F response, there was some indication of a weak 1F response for stimuli containing mid-level properties that are present in the structure of faces. However, this response was much smaller than the response in the face condition, demonstrating that these mid-level properties contribute to, but do not account for the observed contrast asymmetry effect.

4. Discussion

The purpose of the current study was to isolate and compare the high-level responses to positive and negative polarity faces using an objective electrophysiological index recorded over the visual cortex. We observed a first harmonic (1F = 3 Hz) response when a face emerged through progressive increase of its phase coherence. This observation replicates the findings of Ales et al. (2012), even though in the current experiment the same face was repeated during the trials and no explicit behavioral detection task was required. Furthermore, when we alternated between streams of positive and negative polarity faces, we also found evidence of an asymmetrical response that was analogous to the positive polarity response. Finally, we conducted a control experiment which indicated that the asymmetrical response generated by intact faces is almost entirely due to the face-specific structure rather than either low or intermediate feature modulation.

4.1. Dissociation between the perception of positive and negative polarity faces

The first finding of the present study is the presence of a 1F (3 Hz) response to negative contrast polarity faces, reflecting face detection. By itself, the presence of this response implies that negative polarity faces are processed based on more than low-level visual properties (e.g., power spectrum). We observed both similarities and differences in the neural response to positive and negative polarity faces. The 1F response had an occipito-temporal topography in both conditions but the right hemisphere lateralisation was stronger for positive than negative polarity faces, indicating a less distinctive recruitment of high-level and partly face-

specific processes for negative contrast faces. The overall 1F response was also larger for positive compared to negative polarity faces. Moreover, the coherence threshold for the 1F response to negative polarity faces was higher than that for positive polarity faces. Finally, the shape of the 1F response revealed differences in the accumulation of face structure information. Specifically, positive polarity faces elicited a step-like response profile while negative polarity faces elicited a linearly increasing response.

4.1.1. Reduced response amplitudes and increased thresholds for negative polarity faces

A reduction in the overall electrophysiological response at 3 Hz to negative polarity faces is in line with neuroimaging studies in both humans and monkeys, that have reported such reductions in face-selective regions (George et al., 1999; Nasr & Tootell, 2012; Yue et al., 2013) and is also consistent with single-unit recording data from macaque (Ohayon et al., 2012). However, in transient Event-Related Potential (ERP) studies, the face-sensitive N170 component is usually increased rather than decreased by polarity inversion (e.g., Itier & Taylor, 2002), similarly to the effect of picture-plane inversion on this component (Rossion et al., 1999). However, the N170 amplitude decreases to inverted faces when the visibility of the face stimuli is degraded with phase-scrambling (Schneider, DeLong, & Busey, 2007), as in our study. Our findings are therefore compatible with the existing ERP literature.

4.1.2. Qualitatively different sweep response functions for positive vs. negative polarity faces

The 1F response showed distinct profiles for positive compared to negative polarity faces. The step-like profile of positive polarity faces replicates the pattern found in the previous face detection sweep study (Ales et al., 2012) and is similar to previous studies that have parametrically varied the phase coherence of face images (Philiastides & Sajda, 2006; Rousselet et al., 2008). An interesting finding is the linear response function for negative polarity faces that remains smaller in amplitude relative to positive polarity faces, except for the highest levels of coherence. This result is comparable to the only study (Yue et al., 2013) that has, to our knowledge, investigated the effect of contrast polarity on face-related responses while varying face visibility. This is despite some methodological differences (fMRI vs. EEG; RMSE contrast manipulation vs. phase coherence).

Our approach highlights interesting disparities between the processes underlying the detection of positive and negative polar-

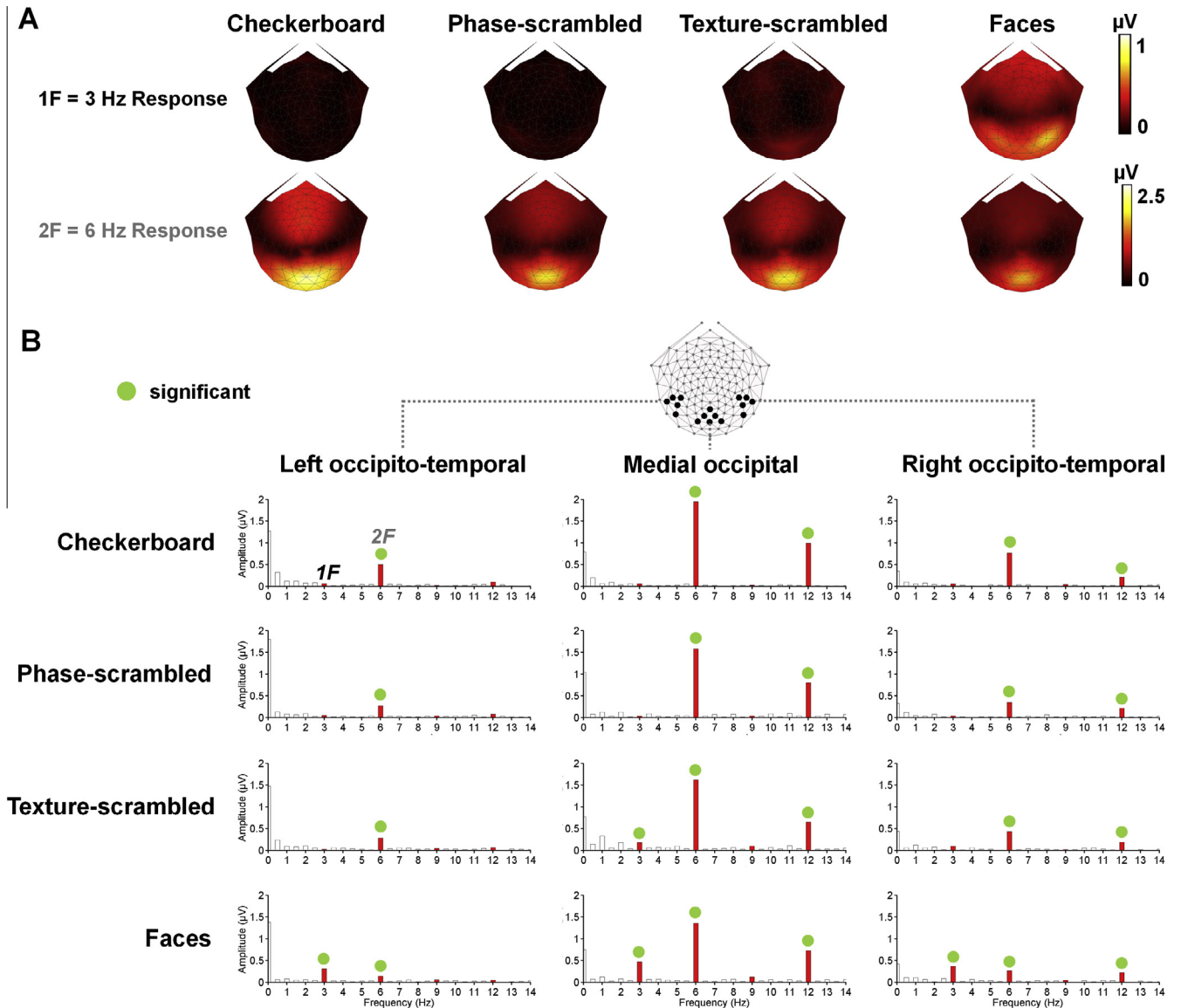


Fig. 6. Topography (A) and frequency spectra (B) of responses across conditions in Section 3. The 1F response is clearly present in the face condition with a strong right lateralisation on the occipito-temporal channels. The texture-scrambled condition also shows some 1F response, though it is weak and localized on the medial occipital channels. At 2F, although the response topography is similar in all conditions, it is much stronger for checkerboard stimuli. Green dots indicate significant responses ($p < 0.05$). (For interpretation of the references to colour in this figure legend, the reader is referred to the web version of this article.)

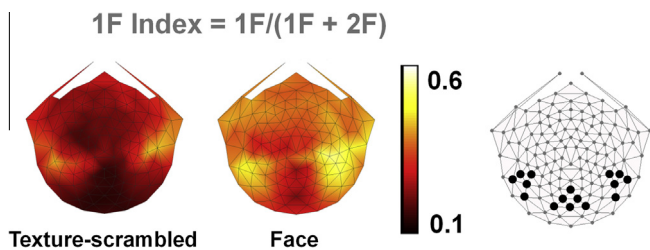


Fig. 7. Topographical distribution of the 1F Index for texture-scrambled and face stimuli.

ity faces. The 1F response indicates that the population response to the face image differs from that of the scrambled image and reflects encoding of the face stimuli at a level of analysis that is beyond that required to process the scrambled image. The step-like function for positive polarity faces suggests the existence of a minimal information threshold for face detection such that any

additional “faceness” input becomes redundant. From a neurofunctional point of view, a minimal amount of “faceness” information may be sufficient to trigger full activation of a population coding for the internal representation of the entire positive polarity face (i.e., a “face template”). Conversely, the linear function for negative polarity faces indicates continued information accumulation. As negative polarity faces are highly unnatural, it is possible that they do not drive the face-selective neural population as efficiently (i.e., no template matching). To test the effect of pre-existing internal representations on 1F response functions, one could compare faces to real-world objects and artificial objects. Hence, if internal representations of real objects can be accessed regardless of polarity, the response 1F response function of real-world objects should be step-like. However, unfamiliar artificial objects seen for the first time should evoke a linear 1F response. In this context, it would also be useful to test potential task effects on these response functions since an explicit face detection or recognition task may change coherence level at which information becomes task-relevant and thus the overall response profile.

4.2. Asymmetry between positive and negative polarity faces

We directly quantified the perceptual asymmetry between positive and negative polarity faces in the polarity reversal condition. We predicted a 1F response only when the response amplitudes of each respective polarity differed the most (i.e., perceived most differently). However, while the 1F response threshold conformed to this linear assumption ($\approx 30\%$ coherence), there was a sustained supra-threshold response that deviated from our predictions at precisely the moment when negative polarity faces should have been detected ($\approx 60\%$ coherence). It would therefore appear that accumulation of face-related information was solely dependent on the positive polarity face stream, despite that the exact same information was present in negative polarity stream. In other words, although faces can be perceived in both streams (i.e., positive and negative polarity conditions), the response to negative polarity faces effectively drops to the same level as EEG noise when directly competing with positive polarity faces.

4.3. Specificity of contrast polarity asymmetry

The second experiment addressed the level of processing at which the contrast polarity reversal effect for faces is first measurable. The traditional contrast reversal response to patterns such as checkerboards or gratings does not generate a first harmonic (e.g., Norcia & Tyler, 1985; Regan, 1973), an effect we replicate here. Exchanges between different exemplars of power-spectrum-matched but phase-scrambled face stimuli did not evoke 1F responses either. This indicates that the scrambling procedure does not create residual luminance artefacts that could generate 1F responses. The third manipulation, scrambling in a way that preserves a level of face-image structure beyond the power spectrum, led to small but statistically significant 1F responses. This last result suggests that the strong response asymmetry to positive and negative faces first occurs at a processing stage when intermediate-level features that are retained by the Portilla–Simoncelli algorithm are encoded. These include correlations across adjacent spatial location, orientation and scales that are present in the intact face image.

The contrast polarity asymmetry is thought to be specific to faces. For instance, there is only a small or non-existent reduction of discrimination performance for negative polarity versions of real (i.e., dogs, Robbins & McKone, 2007; chairs, Itier, Latinus, & Taylor, 2006), artificial (i.e., “Greebles”; Vuong et al., 2005), or abstract visual objects (i.e., “blobs”, Nederhouser et al., 2007; Yue et al., 2013). Although one can argue that only a limited number of object categories have been tested, the consistency of the contrast polarity effect with a wide variety of “face” stimuli points towards specificity. More specifically, the deleterious effect of contrast negation has been demonstrated with realistic faces of different degrees of familiarity (unfamiliar, e.g., Liu et al., 1999; famous, e.g., Gilad, Meng, & Sinha, 2008; personally familiar, e.g., Bruce & Langton, 1994; experimentally familiarised, e.g., Galper, 1970) to simplified two-tone faces (i.e., Mooney faces, George et al., 1999; Otsuka et al., 2012; Phillips, Jenkins, & Morris, 1972) and even schematic stimuli arranged in a crude face-like configuration (i.e., two eyes and a mouth, Tomalski et al., 2009; Farroni et al., 2005). Both infant preference (Farroni et al., 2005; Otsuka et al., 2012) and monkey neurophysiology (Ohayon et al., 2012) show that positive contrast polarity is essential to elicit a preferential response for face/face-like stimuli. An interesting question would be whether the stimulus needs to be perceived as a face in order to show sensitivity to contrast polarity. This could be addressed by using ambiguous stimuli primed to be seen as a face or as a non-face, or by contrast-reversing stimuli that parametrically increase in their “facedness”. The current experiment cannot answer this question, since

the emergence of a face is confounded with the emergence of structure (i.e., scrambled vs. unscrambled).

4.4. Origins of contrast polarity effect

Two main theories regarding the origins of the contrast polarity effect have debated whether contrast negation disrupts visual cues related to the estimation of shape from shading (Kemp et al., 1996; Lewis & Johnston, 1997; Liu et al., 1999; Liu, Collin, & Chaudhuri, 2000) or the perception of surface texture/pigmentation (Bruce & Langton, 1994; Nederhouser et al., 2007; Russell et al., 2006). Lighting direction also appears to play a role since negative polarity faces resemble bottom-lit faces, which are harder to recognise (Johnston, Hill, & Carman, 1992; Liu et al., 1999; Liu, Collin, & Chaudhuri, 2000). More recently, contrast polarity effects have been considered in terms of the relative contrast pattern in a face (i.e., eyes darker than forehead) rather than absolute luminance values (Dakin & Watt, 2009; Gilad, Meng, & Sinha, 2008; Ohayon et al., 2012). Eliminating this dark-vs.-light pattern via equiluminance (Pearce & Arnold, 2013) or inverting it in a key region such as the eyes drastically impair face perception (Gilad, Meng, & Sinha, 2008; Sormaz, Andrews, & Young, 2013). This view could explain contrast polarity effects across a variety of face stimuli that lack shading, lighting, or pigmentation cues (i.e., two-tone Mooney faces, schematic faces) and generalises the effects beyond face discrimination to face perception. Contrast patterns are most salient at low and medium spatial frequencies (i.e., cycles per face) and, accordingly, contrast polarity effects are largest in these frequency bands (Hayes, 1988; Hayes, Concetta Morrone, & Burr, 1986). Interestingly, newborns and infants show contrast polarity effects and have access only to low-medium spatial frequency vision (Acerra, Burnod, & de Schonen, 2002; De Heering et al., 2008). Sensitivity to contrast polarity may therefore result from a conjunction between developmental visual constraints and real-world face statistics. Since the sweep VEP is a powerful technique to investigate visual processing in developmental populations thanks to the speed and objectivity with which responses can be acquired (e.g., Almoqbel, Leat, & Irving, 2008; Farzin, Hou, & Norcia, 2012; Norcia & Tyler, 1985), this approach could be implemented to test the contrast polarity effect across development.

Acknowledgments

This research was funded by a grant from the European Research Council (facessvep 284025) awarded to B.R. and a travel Grant from the Belgian National Scientific Research Fund (A2/5-ROI/JA-1240) awarded to J.L.-S. The authors would like to thank Faraz Farzin and Claudia Arrighi for their help for data acquisition and participant recruitment, Vladimir Vildavski for helpful comments regarding data analysis, and Bastien Gorissen for providing the function fitting scripts.

Appendix A. Supplementary data

Supplementary data associated with this article can be found, in the online version, at <http://dx.doi.org/10.1016/j.visres.2015.01.001>.

References

- Acerra, F., Burnod, Y., & de Schonen, S. (2002). Modelling aspects of face processing in early infancy. *Developmental Science*, 5, 98–117.
- Ales, J. M., Farzin, F., Rossion, B., & Norcia, A. M. (2012). An objective method for measuring face detection using the sweep steady-state visual evoked response. *Journal of Vision*, 12, 18.
- Almoqbel, F., Leat, S. J., & Irving, E. (2008). The technique, validity and clinical use of the sweep VEP. *Ophthalmic and Physiological Optics*, 28, 393–403.

- Bentin, S., McCarthy, G., Perez, E., Puce, A., & Allison, T. (1996). Electrophysiological studies of face perception in humans. *Journal of Cognitive Neuroscience*, 8, 551–565.
- Bruce, V., & Langton, S. (1994). The use of pigmentation and shading information in recognising the sex and identities of faces. *Perception*, 23, 803–822.
- Carlson, T., Grol, M. J., & Verstraten, A. J. (2006). Dynamics of visual recognition revealed by fMRI. *NeuroImage*, 32, 892–905.
- Crouzet, S. M., Kirchner, H., & Thorpe, S. J. (2010). Fast saccades toward faces: Face detection in just 100 ms. *Journal of Vision*, 10(16), 1–17.
- Crouzet, S. M., & Thorpe, S. J. (2011). Low-level cues and ultra-fast face detection. *Frontiers in Psychology*, 2(342), 1–9.
- Dakin, S. C., & Watt, R. J. (2009). Biological “bar codes” in human faces. *Journal of Vision*, 9, 1–10.
- De Heering, A., Turati, C., Rossion, B., Bulf, H., Goffaux, V., & Simion, F. (2008). Newborns’ face recognition is based on spatial frequencies below 0.5 cycles per degree. *Cognition*, 106, 444–454.
- Farroni, T., Johnson, M. H., Menon, E., Zulian, L., Faraguna, D., & Csibra, G. (2005). Newborns’ preference for face-relevant stimuli: Effects of contrast polarity. *PNAS*, 102, 17245–17250.
- Farzin, F., Hou, C., & Norcia, A. M. (2012). Piecing it together: Infants’ neural responses to face and object structure. *Journal of Vision*, 12, 6.
- Galper, R. E. (1970). Recognition of faces in photographic negative. *Psychonomic Science*, 19, 207–208.
- George, N., Dolan, R. J., Fink, G. R., Baylis, G. C., Russell, C., & Driver, J. (1999). Contrast polarity and face recognition in the human fusiform gyrus. *Nature Neuroscience*, 2, 574–580.
- Gilad, S., Meng, M., & Sinha, P. (2008). Role of ordinal contrast relationships in face encoding. *PNAS*, 106, 5353–5358.
- Hayes, A. (1988). Identification of two-tone images; some implications for high- and low-spatial-frequency processes in human vision. *Perception*, 17, 429–436.
- Hayes, T., Concetta Morrone, M., & Burr, D. C. (1986). Recognition of positive and negative bandpass-filtered images. *Perception*, 15, 595–602.
- Hou, C., Good, W. V., & Norcia, A. M. (2007). Validation study of VEP Vernier acuity in normal-vision and amblyopic adults. *IOVS*, 48, 4070–4078.
- Itier, R. J., Latinus, M., & Taylor, M. J. (2006). Face, eye and object early processing: What is the face specificity? *NeuroImage*, 29, 667–676.
- Itier, R. J., & Taylor, M. J. (2002). Inversion and contrast polarity reversal affect both encoding and recognition processes of unfamiliar faces: A repetition study using ERPs. *NeuroImage*, 15, 353–372.
- James, T. W., Humphrey, G. K., Gati, J. S., Menon, R. S., & Goodale, M. A. (2000). The effects of visual object priming on brain activation before and after recognition. *Current Biology*, 10, 1017–1024.
- Jemel, B., Schuller, A.-M., Cheref-Khan, Y., Goffaux, V., Crommelinck, M., & Bruyer, R. (2003). Stepwise emergence of the face-sensitive N170 event-related potential component. *NeuroReport*, 14, 2035–2039.
- Jiang, F., Dricot, L., Weber, J., Righi, G., Tarr, M. J., Goebel, R., et al. (2011). Face categorization in visual scenes may start in a higher order area of the right fusiform gyrus: Evidence from dynamic visual stimulation in neuroimaging. *Journal of Neurophysiology*, 106, 2720–2736.
- Johnston, A., Hill, H., & Carman, N. (1992). Recognising faces: Effects of lighting direction, inversion, and brightness reversal. *Perception*, 21, 365–375.
- Keil, M. S. (2008). Does face image statistics predict a preferred spatial frequency for human face processing? *Proceedings of the Royal Society: Biological Sciences*, 275, 2095–2100.
- Kemp, R., Pike, G., White, P., & Musselman, A. (1996). Perception and recognition of normal and negative faces: Role of shape from shading and pigmentation. *Perception*, 25, 37–52.
- Lewis, M. B., & Edmonds, A. J. (2003). Face detection: Mapping human performance. *Perception*, 32, 903–920.
- Lewis, M. B., & Edmonds, A. J. (2005). Searching for faces in scrambled scenes. *Visual Cognition*, 12, 1309–1336.
- Lewis, M. B., & Johnston, R. A. (1997). The Thatcher illusion as a test of configural disruption. *Perception*, 26, 225–227.
- Liu, C. H., Collin, C. A., Burton, A. M., & Chaudhuri, A. (1999). Lighting direction affects recognition of untextured faces in photographic positive and negative. *Vision Research*, 39, 4003–4009.
- Liu, C. H., Collin, C. A., & Chaudhuri, A. (2000). Does face recognition rely on encoding of 3-D surface? Examining the role of shape-from-shading and shape-from-stereo. *Perception*, 29, 729–743.
- Maris, E., & Oostenveld, R. (2007). Nonparametric statistical testing of EEG- and MEG-data. *Journal of Neuroscience Methods*, 164, 177–190.
- Nasr, S., & Tootell, R. B. H. (2012). Role of fusiform and anterior temporal cortical areas in facial recognition. *NeuroImage*, 63, 1743–1753.
- Nederhouser, M., Yue, X., Mangini, M. C., & Biederman, I. (2007). The deleterious effect of contrast reversal on recognition is unique to faces, not objects. *Vision Research*, 47, 2134–2142.
- Norcia, A. M., & Tyler, C. W. (1985). Spatial frequency sweep VEP: Visual acuity during the first year of life. *Vision Research*, 25, 1399–1408.
- Norcia, A. M., Tyler, C. W., & Hamer, R. D. (1990). Development of contrast sensitivity in the human infant. *Vision Research*, 30, 1475–1486.
- Ohayon, S., Freiwald, W. A., & Tsao, D. Y. (2012). What makes a cell face selective? The importance of contrast. *Neuron*, 74, 567–581.
- Otsuka, Y., Hill, H. C. H., Kanazawa, S., Yamaguchi, M. K., & Spehar, B. (2012). Perception of Mooney faces by young infants: The role of local feature visibility, contrast polarity, and motion. *Journal of Experimental Child Psychology*, 111, 164–179.
- Paras, C. L., & Webster, M. A. (2013). Stimulus requirements for face perception: An analysis based on “totem poles”. *Frontiers in Psychology*, 4(18), 1–16.
- Pearce, S. L., & Arnold, D. H. (2013). Facial coding is disrupted at equiluminance. *Perception*, 42, 835–848.
- Pei, F., Pettet, M. W., & Norcia, A. M. (2007). Sensitivity and configuration-specificity of orientation-defined texture processing in infants and adults. *Vision Research*, 47, 338–348.
- Philiastides, M. G., Ratcliff, R., & Sajda, P. (2006). Neural representation of task difficulty and decision making during perceptual organization: A timing paradigm. *Journal of Neuroscience*, 26, 8965–8975.
- Philiastides, M. G., & Sajda, P. (2006). Temporal characterization of the neural correlates of perceptual decision making in the human brain. *Cerebral Cortex*, 16, 509–518.
- Phillips, R. J., Jenkins, R., & Morris, D. (1972). Why are faces hard to recognize in photographic negative? *Perception & Psychophysics*, 12, 425–426.
- Portilla, J., & Simoncelli, E. P. (2000). A parametric texture model based on joint statistics of complex wavelet coefficients. *International Journal of Computer Vision*, 40, 49–71.
- Regan, D. (1966). Some characteristics of average steady-state and transient responses evoked by modulated light. *Electroencephalography and Clinical Neurophysiology*, 20, 238–248.
- Regan, D. (1973). Rapid objective refraction using evoked brain potentials. *Investigative Ophthalmology*, 12, 669–679.
- Regan, D. (1989). *Human brain electrophysiology: Evoked potentials and evoked magnetic fields in science and medicine*. New York: Elsevier.
- Reinders, A. A. T. S., den Boer, J. A., & Büchel, C. (2005). The robustness of perception. *European Journal of Neuroscience*, 22, 524–530.
- Robbins, R., & McKone, E. (2007). No face-like processing for objects-of-expertise in three behavioural tasks. *Cognition*, 103, 34–79.
- Rolls, E. T., & Baylis, G. C. (1986). Size and contrast have only small effects on the response to faces of neurons in the cortex of the superior temporal sulcus of the monkey. *Experimental Brain Research*, 65, 38–48.
- Rossion, B., & Jacques, C. (2011). The N170: Understanding the time-course of face perception in the human brain. In S. Luck, E. Kappenman (Eds.), *The Oxford handbook of ERP components*. Oxford University Press.
- Rossion, B., & Boremanse, A. (2011). Robust sensitivity to facial identity in the right human occipito-temporal cortex as revealed by steady-state visual-evoked potentials. *Journal of Vision*, 16, 1–21.
- Rossion, B., Delvenne, J.-F., Debatisse, D., Goffaux, V., Bruyer, R., Crommelinck, M., et al. (1999). Spatio-temporal brain localization of the face inversion effect. *Biological Psychology*, 50, 173–189.
- Rousselet, G. A., Pernet, C. R., Bennett, P. J., & Sekuler, A. B. (2008). Parametric study of EEG sensitivity to phase noise during face processing. *BMC Neuroscience*, 9, 98.
- Russell, R., Sinha, P., Biederman, I., & Nederhouser, M. (2006). Is pigmentation important for face recognition? Evidence from contrast negation. *Perception*, 35, 749–759.
- Schneider, B. L., DeLong, J. E., & Busey, T. A. (2007). Added noise affects the neural correlates of upright and inverted faces differently. *Journal of Vision*, 7, 1–24.
- Sormaz, M., Andrews, T. J., & Young, A. W. (2013). Contrast negation and the importance of the eye region for holistic representations of facial identity. *Journal of Experimental Psychology: Human Perception and Performance*, 36, 1667–1677.
- Tang, Y., & Norcia, A. M. (1995). An adaptive filter for steady-state evoked responses. *Electroencephalography and Clinical Neurophysiology*, 96, 268–277.
- Tanskanen, T., Näsänen, R., Montez, T., Päällysaho, J., & Hari, R. (2005). Face recognition and cortical responses show similar sensitivity to noise spatial frequency. *Cerebral Cortex*, 15, 526–534.
- Tomalski, P., & Johnson, M. H. (2012). Cortical sensitivity to contrast polarity and orientation of faces is modulated by temporal-nasal hemifield asymmetry. *Brain Imaging and Behavior*, 6, 88–101.
- Tyler, C. W., Apkarian, P., Levi, D. M., & Nakayama, K. (1979). Rapid assessment of visual function: An electronic sweep technique for the pattern visual evoked potential. *Investigative Ophthalmology & Visual Science*, 18, 703–713.
- Vuong, Q. C., Peissig, J. J., Harrison, M. C., & Tarr, M. J. (2005). The role of surface pigmentation for recognition revealed by contrast reversal in faces and Greebles. *Vision Research*, 45, 1213–1223.
- Willenbockel, V., Sadr, J., Fiset, D., Horne, G. O., Gosselin, F., & Tanaka, J. W. (2010). Controlling low-level image properties: The SHINE toolbox. *Behavior Research Methods*, 42, 671–684.
- Yue, X., Nasr, S., Devaney, K. J., Holt, D. J., & Tootell, R. B. H. (2013). fMRI analysis of contrast polarity in face-selective cortex in humans and monkeys. *NeuroImage*, 76, 57–69.